Supplemental Document

Biomedical Optics EXPRESS

Quantitative and anatomical imaging of dermal angiopathy by noninvasive photoacoustic microscopic biopsy: supplement

Haigang Ma,[1,2,3] Zhongwen Cheng,[1,4] Zhiyang Wang,[1,4] Haixia Qiu,[5] Tianding Shen,[6] Da Xing,[1,4] Ying Gu,[5,7] and Sihua Yang[1,4,*]

[1] *MOE Key Laboratory of Laser Life Science and Institute of Laser Life Science, College of Biophotonics, South China Normal University, Guangzhou 510631, China*
[2] *Shenzhen Research Institude of Northwestern Polytechnical University, Shenzhen 518057, China*
[3] *School of Artificial Intelligence, Optics and Electronics (iOPEN), Northwestern Polytechnical University, Xi'an 710072, China*
[4] *Guangdong Provincial Key Laboratory of Laser Life Science, College of Biophotonics, South China Normal University, Guangzhou 510631, China*
[5] *Department of Laser Medicine, First Medical Center of PLA General Hospital, Beijing 100853, China*
[6] *Department of Plastic and Aesthetic Surgery, Nanfang Hospital, Southern Medical University, Guangzhou 510515, China*
[7] *guyinglaser@sina.com*
[*] *yangsh@scnu.edu.cn*

Supplement DOI: https://doi.org/10.6084/m9.figshare.16592918

Parent Article DOI: https://doi.org/10.1364/BOE.439625

Quantitative and anatomical imaging of dermal angiopathy by noninvasive photoacoustic microscopic biopsy: supplemental document

Haigang Ma[1,5,6], Zhongwen Cheng[1,2], Zhiyang Wang[1,2], Haixia Qiu[3], Tianding Shen[4], Da Xing[1,2], Ying Gu[3,7] and Sihua Yang[1,2*]

[1]MOE Key Laboratory of Laser Life Science & Institute of Laser Life Science, College of Biophotonics, South China Normal University, Guangzhou 510631, China.

[2]Guangdong Provincial Key Laboratory of Laser Life Science, College of Biophotonics, South China Normal University, Guangzhou 510631, China.

[3]Department of Laser medicine, First medical center of PLA General Hospital, Beijing 100853, China.

[4]Department of Plastic and Aesthetic Surgery, Nanfang Hospital, Southern Medical University, Guangzhou 510515, China.

[5]shenzhen Research Institude of Northwestern Polytechnical University, Shenzhen 518057, China.

[6]School of Artificial Intelligence, Optics and Electronics (iOPEN), Northwestern Polytechnical University, Xi'an 710072 , China.

[7]guyinglaser@sina.com

*yangsh@scnu.edu.cn

Supplementary Notes

Note S1. Description of noninvasive photoacoustic microscopic biopsy (PAMB) system.

Fig. S1a shows a scheme of the photoacoustic microscopic biopsy (PAMB) elements, their connections. A miniature laser (Model DTL-314QT, pulsed Q-switched laser, Russia) operating at a 4-ns pulse width at 532-nm with a 10-kHz repetition rate is used as the radiation source. The miniature laser is focused by a convex lens, which passes through a 25-μm pinhole for spatial filtering. The laser is then coupled into a single-mode fibre using a plan objective lens [numerical aperture (NA) of 0.1, working distance (WD) of 37.5 mm], and guided into a scalable confocal opto-sono objective (**Fig. S1b**). Finally, the scalable confocal opto-sono objective is used to focus the exited spot and irradiate the test-area to produce PA signals. The core parts of the scalable confocal opto-sono objective are the switchable objective lenses, which can switch between different NAs (typically 4×/0.1, 10×/0.3, and 20×/0.55, **Fig. S1c and 1d**), a multiscale adjustable device with a large depth-adjustable range of focus (0–3 cm), and a hollow spherically focused Polyvinylidene Fluoride (PVDF) transducer. The PVDF transducer has an overall diameter of 4-mm with a 1-mm centre hole that allows the laser beam to exit. Typical focal length is 14.3-mm, generated by the spherically focused structure, producing a NA of 0.28 (central frequency of the PVDF transducer is 42 MHz). The collected PA signals are sequentially pre-amplified with a 50 dB low noise amplifier (LNA-650, RF Bay, Inc., USA) that is digitised using a dual-channel data acquisition card (M4i.4450-x8, Spectrum, German). The opto-sono objective is actuated automatically by a two-dimensional scanner (scan distance of 5 × 5 cm^2, scan resolution of 0.1-μm, HRXWJ-50R-2, Beijing TianRuiZhongHai Precision instrument Co., Ltd, China). The scanning range of the PAMB is 0.5 × 0.5 to 20 × 20 mm^2.

Note S2. The resolution and imaging depth of the PAMB system.

The lateral resolution of PAMB with three objective lenses (4×/0.1 NA, 10×/0.3 NA, and 20×/0.55 NA) was measured by imaging a sharp-edged surgical blade. The fitted edge-spread function (ESF) was estimated from the blade PA data along the white dashed line at the focal distance. The line-spread function (LSF) was calculated as the derivative of the ESF. The full width at half-maximum (FWHM) of the LSF was respectively estimated as 3.8 μm, 2.3 μm, and 1.5 μm under the three NA modes (**Fig. S2a**). The axial resolution of the system depends primarily on the acoustic prameter, which is estimated as ~34 μm based on the system bandwidth and acoustic speed within tissue (**Fig. S2b**). In view of the dermal microvasculature assessment of port wine stains by PAMB with the 4×/0.1 NA mode, the imaging depth of PAMB system was measured in the 4 ×/0.1 NA mode, and thus a black human hair (diameter, 120 μm) was obliquely inserted into a phantom and imaged. This analysis demonstrated that the imaging depth is approximately 3 mm (**Fig. S2c**).

Note S3. PA mapping of port wine stain (PWS) skin in central and lateral facial locations.

The study was performed to demonstrate the PAMB could resolve and quantify features of PWS in different locations. Central facial PWS skin areas were imaged in one Asiatic patient with PWS (**Fig. S3a**), revealing marked changes compared with lateral facial PWS skin that from the same patient (**Fig. S3b**). This was further confirmed by the statistics, i.e., average vascular diameter, depth and density from the central and lateral facial PWS skin of the same patient, as shown in **Fig. S3c**.

Finally, 20 volunteers with central and lateral facial PWS skin were randomly selected, aged 5–50 years, and statistically assessed the average vascular diameter, depth, and density of the central and the lateral facial PWS skin, respectively. The results indicate that the average vascular diameter, depth and density of central facial PWS skin are greater than those of lateral facial PWS skin (**Fig. S3, d to f**). Significant differences in the vascular morphology of PWS skin were noted between central facial PWS skin and lateral facial PWS skin from the same PWS patient.

Note S4. PA mapping of PWS skin at different stages.

The study was performed to investigate PAMB could resolve and quantify features of PWS at different stages. We imaged the affected areas (3 mm × 3 mm) on the skin of three patients with PWS at different stages (pink, purple, and proliferative, **Fig. S4a**). Then ten patients with each stage of PWS were selected at random. Lesion vessel depth and density of central facial PWS skin were statistically assessed. The results revealed significant differences ($P < 0.01$) in the lesion vessel depth and density between PWS lesions at different stages (**Fig. S4b**).

Note S5. Clinical trials of 174 Asian PWS patients.

The study was performed to evaluate the effectiveness and reliability of the PAMB for 174 PWS patients. In this single-center, cross-sectional diagnostic study (Clinical Trials. gov numbers, 2017 Ethic Review No. 012 and NFEC-2017-093), the PAMB was used to perform preoperative assessment of dermal vascular malformations for 174 patients with PWS skin disease in First medical center of PLA General Hospital and Nanfang Hospital of Southern Medical University. Before skin imaging, verbal and written informed consent was obtained from 174 Asian PWS volunteers. Patients' conditions and photoacoustic imaging data were evaluated by the three experienced pathologists to confirm the clinical diagnosis. Then the morphological features (average density, average diameter, maximum diameter, average depth, and maximum depth) of vessels between PWS skin and healthy skin from the 174 patients (gender, age, and weight were compared in **Tables S1 and S2**) were compared by PAMB, respectively, which was determined on the basis of clinical scoring. Statistical result displayed that the density of the vessels (average vessel/skin area ratio) in PWS skin (14.50±1.86%) was higher than that in healthy skin (2.47±1.05%). After paired *t* test, $t = 13.17$, and $P = 0.00 < 0.05$ (**Table S3**); the average diameter of the vessels in PWS skin (109.14±10.72 μm) was larger than that in healthy skin (22.47±2.36 μm). After paired *t* test, $t = 17.64$, and $P = 0.00 < 0.05$ (**Table S4**); the maximum diameter of the vessels in PWS skin (138.52±14.51 μm) was larger than that in healthy skin (31.53±5.36 μm). After paired *t* test, $t = 21.51$, and $P = 0.00 < 0.05$ (**Table S5**); the average depth of the vessels in PWS skin (615.00±195.00μm) was larger than that in healthy skin (430.00±160.00 μm). After paired *t* test, $t = 19.00$, and $P = 0.00 < 0.05$ (**Table S6**); and the maximum depth of the vessels in PWS skin (760.00±235.00 μm) was larger than that in healthy skin (510.00±185.00 μm). After paired *t* test, $t = 21.46$, and $P = 0.00 < 0.05$ (**Table S7**). It can be considered that the average density, average diameter, maximum diameter, average depth, and maximum depth of vessels between PWS skin and healthy skin from the 174 patients have statistical

significance. Meantime, the morphological features (average density, average diameter, maximum diameter, average depth, and maximum depth) of vessels from three color types of clinical manifestations (63 pink PWS patients, 59 purple PWS patients, and 52 proliferative PWS patients were shown in **Table S8**) of 174 PWS patients were compared using clinical PAMB data, respectively. Statistical result displayed that the average densities of the vessels from pink PWS skin, purple PWS skin, and proliferative PWS skin were 6.71±0.87%, 14.69±1.18%, and 23.73±2.46% (**Table S9**); the average diameters of the vessels from pink PWS skin, purple PWS skin, and proliferative PWS skin were 68.39±10.51 μm, 113.35±12.53 μm, and 153.72±17.81 μm (**Table S10**); the maximum diameters of that were 94.51±12.16 μm, 141.36±15.08 μm, and 178.69±19.75 μm (**Table S11**); and the average depths of the vessels from pink PWS skin, purple PWS skin, and proliferative PWS skin were 455±185 μm, 570±190 μm, and 865±210 μm (**Table S12**); the maximum depths of that were 580±210 μm, 740±220 μm, and 1080±240 μm (**Table S13**), respectively. The results can be considered that the average diameter of vessels in the PWS and healthy skin from pink PWS skin, purple PWS skin, and proliferative skin, the maximum diameter of that, and the number of that have significant difference.

Note S6. Medical procedures for the PA skin imaging.

The medical procedures were performed for human skin imaging as follows: firstly, the PA scanning head was flexibly attached to a mechanical arm to control over the relative position between the objective and the skin surface. Secondly, before each experiment, the volunteer rested in the temperature-controlled laboratory (at 20°C) for 15 min to adapt to the environmental temperature. The imaged skin area was cleaned with alcohol swabs, and then was coated with a thin layer of conventional medical ultrasonic coupling agent. Finally, for the data acquisition process, the PA scanning head was placed on surface of the imaged skin area, and then scanned perpendicular to its axial axis, conformed a rectangular grid parallel to the skin surface. In skin imaging, we used a laser with a repetition rate of 10 kHz, so the image uniform acquisition time is approximately 0.5 s for a ~5 mm B-Scan PA imaging area with a scanning step of 1 μm. The PA signals were averaged 10 times, and the separation distance between each B-scan image was 10 μm. For the human skin experiments, all human skin images were generated using PA signals collected over 5mm × 5 mm (scan points, 500 × 500), taking an acquisition time of ~2.5 min per PA image. The entire volunteer handling process, including placement of the PAM on the skin tissue surface lasted less than 3-4 min. The total experimental time spent on the volunteer was <1.5 h, including rested every 20 min to prevent numbness of the extremities.

Supplementary Figures

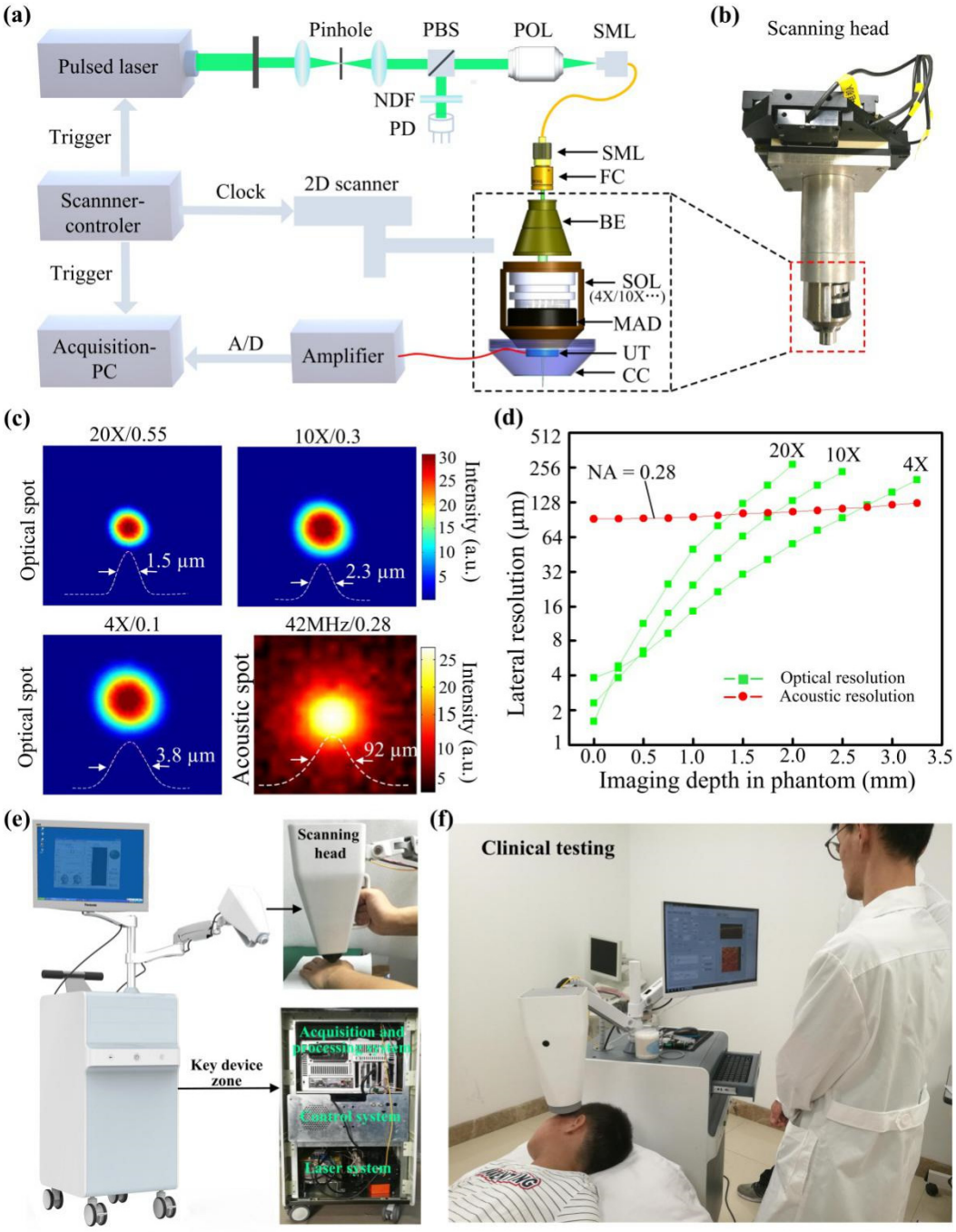

Fig. S1. PAMB system using a scalable confocal opto-sono objective. (a) Schematic of the entire system. NDF, neutral density filter; PBS, polarising beam splitter; PD,

photodiode; POL, plan objective lens; SMF, single-mode fibre; FC, fibre collimator; BE, beam expander; SOL, switchable objective lenses; MAD, multiscale adjustable device; UT, ultrasound transducer; CC, coupling cup. (b) Photo of the scanning head. (c) Intensity profiles of optical spots (three NA modes: 4×/0.1, 10×/0.3, and 20×/0.55) and an acoustic spot at the focal distance (42 MHz/0.28). (d**)** Variation diagram of the lateral resolution as the focal depth position in a phantom. The phantom was made of agarose, intralipid, and India ink, which had similar optical characteristics (an optical absorption coefficient of ~0.01 mm^{-1} and a reduced scattering coefficient of ~1.0 mm^{-1}) and acoustic feature (an acoustic impedance of ~1.5 MRayl) with human skin tissue. (e) Photographs of the PAMB system, the key device zone, and the scanning head in position. (f) Clinical testing of PAMB system in one Asiatic patient with port wine stains (PWS).

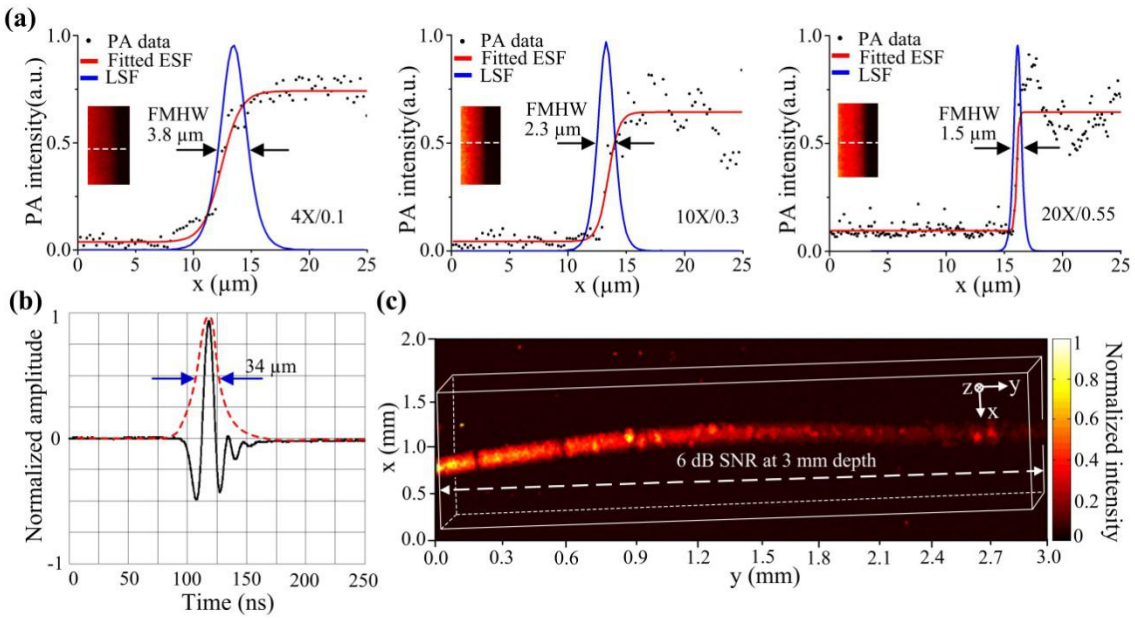

Fig. S2. System characteristics of PAMB system. (a) Estimation of the lateral resolution with multiple objective lenses (typically: 4×/0.1 NA; 10×/0.3 NA; 20×/0.55 NA) by imaging a sharp-edged surgical blade. The LSF was obtained by taking the derivative of the ESF, which was extracted from the PA image of a sharp edge. (b) Pulse response of the opto-sono objective at the focus point (black line). The red dotted line is the corresponding Hilbert-transformed envelope. The axial resolution can be considered to be the full width at half maximum (FWHM) of the envelope, which is approximately 34 μm. (c) Imaging depths of PAMB. Hair was imaged using PAMB with an SNR of ≥ 6 dB up to a depth of ~3 mm in a phantom.

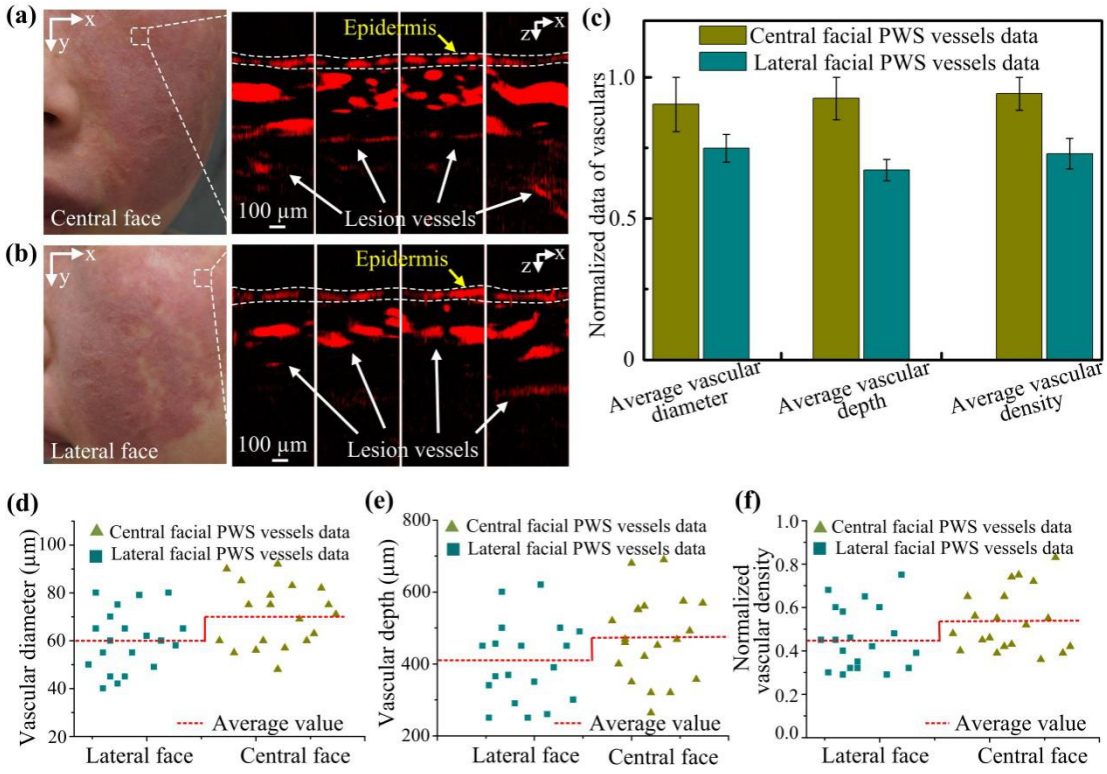

Fig. S3. PA mapping of PWS skin at different positions by PAMB. (a and b) Photographs of one Asiatic patient (11-year-old girl with a purple lesion) with PWS skin in different positions of the face (central and lateral) and consecutive cross-sectional PA images of the different positions. (c) Statistics (average vascular diameter, average vascular depth and vascular density) from PA images of the detection areas in (a and b) using the ImageJ software. (d to f) The average vascular diameter, depth and density of central facial PWS skin versus that of lateral facial PWS skin (n = 20).

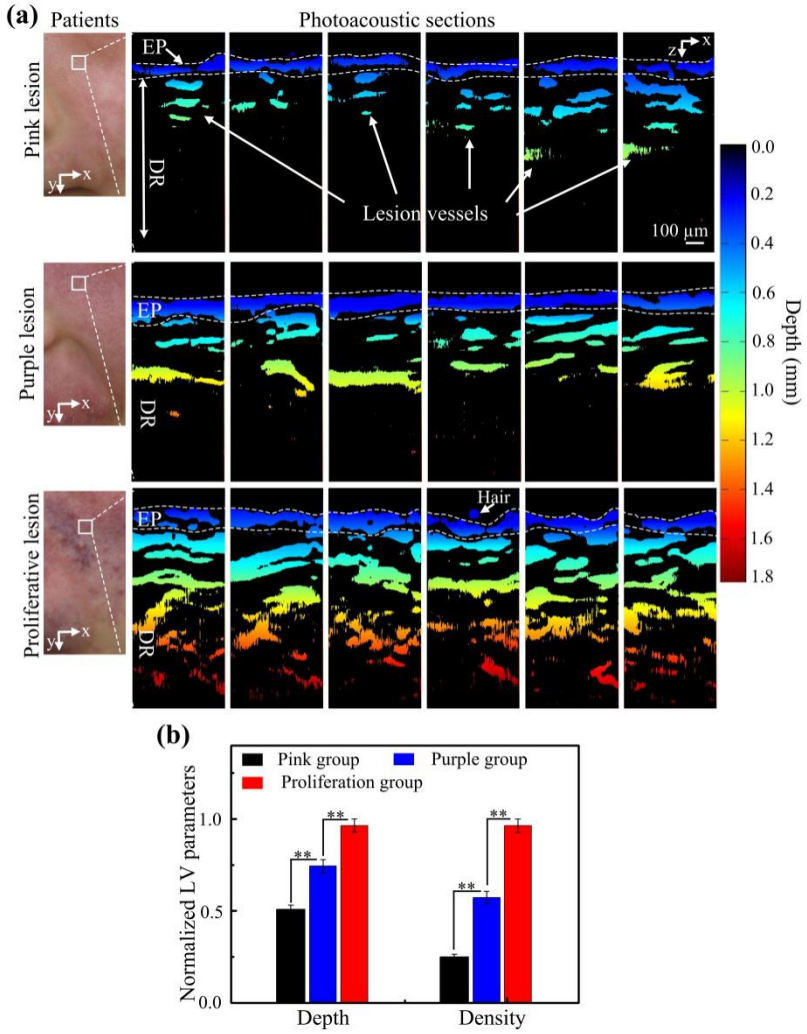

Fig. S4. PA mapping of PWS skin at different stages by PAMB. (a) Photographs of the skin of three patients with PWS at different stages (pink lesion, purple lesion, or proliferative lesion) and consecutive cross-sectional photoacoustic images of human faces. Simultaneously, the cross-sectional images appeared in the counterpart depth encode images, which are more intuitive for displaying the spatial distribution of lesion vessels. Demographic data of the three patients (respectively): (1) PWS stage: pink lesion, purple lesion, and proliferative lesion; (2) age: 7, 15, and 41 years; (3) gender: male, female, female. (b) Average lesion vessel (LV) depth and LV density statistics were obtained from the photoacoustic images of patients with PWS at different stages (n = 10 per group, $^{**}p < 0.01$).

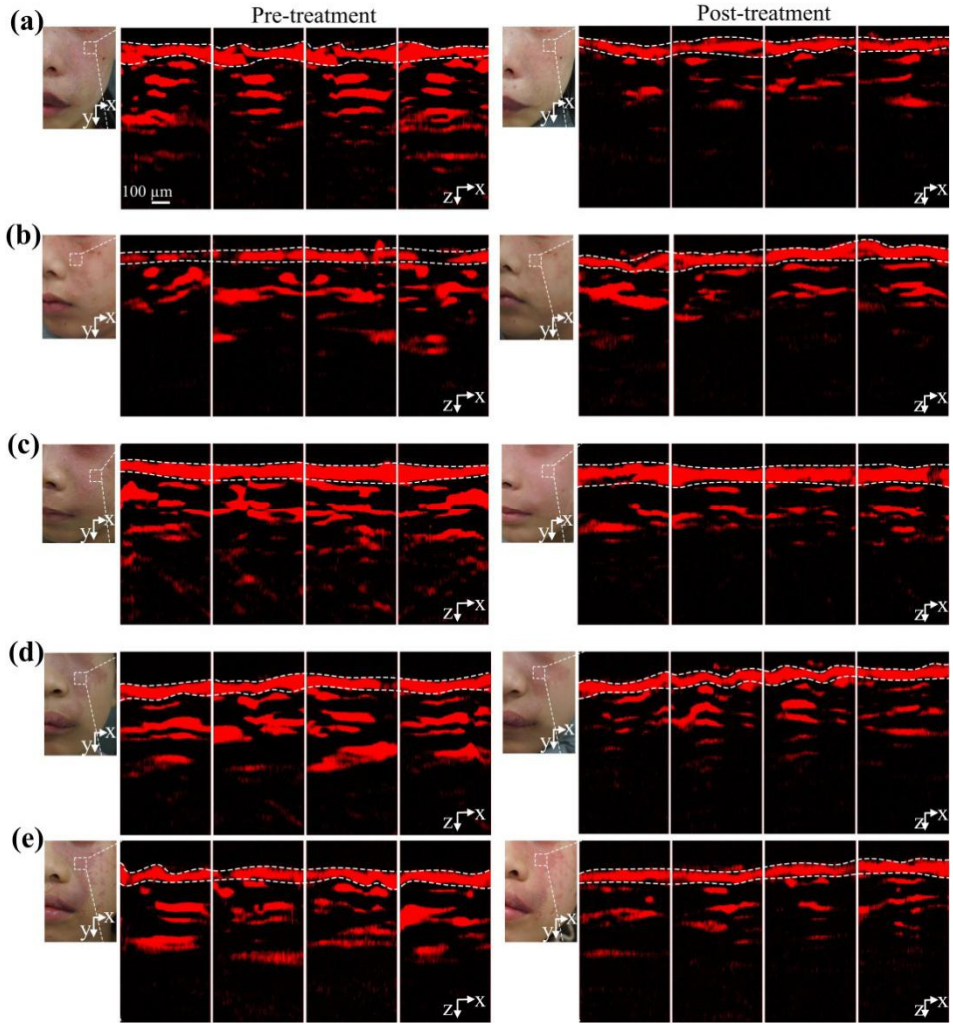

Fig. S5. Evaluating curative effect of photodynamic therapy (PDT) by PAMB. (a to e) Photographs and consecutive cross-sectional photoacoustic images of PWS skin before and after PDT treatment from five volunteers. The demographic information of the three volunteers, respectively, is as follows: 7, 12, 10, 8, and 10 year old; female, male, male, female, female; pink lesion, pink lesion, pink lesion, purple lesion, and purple lesion.

Supplementary Tables

Table S1. Demography characteristics for 174 PWS patients

Characteristics	Result
Sex	
Male	61 (35.06%)
Female	113 (64.94%)
Sum	174
Age (year)	
N (Missing)	174 (0)
Average (SD)	15.85 (9.51)
Min, Max	5.00, 48.00
Md (Q3-Q1)	24.00 (12.50)
Weight (Kg)	
N (Missing)	74(0)
Average (SD)	38.15 (16.15)
Min, Max	23.00, 93.00
Md (Q3-Q1)	42.00 (20.50)

Note: N, number of PWS patients; SD, standard deviation; Md, median, Q1, first quartile; Q3, third quartile.

Table S2. Age and weight were compared by gender for 174 PWS patients

Characteristics	Male	Female	Test statistic	*P* value
Age (year)				
N (Missing)	61 (0)	113 (0)	-1.01 (*t* value)	0.3159
Average (SD)	14.76 (5.59)	6.44 (6.88)		
Min, Max	5.00, 48.00	5.00, 44.00		
Md (Q3-Q1)	23.00 (14.00)	24.00 (12.00)		
Weight (kg)				
N (Missing)	61 (0)	113 (0)	11.07 (*t* value)	0.0000
Average (SD)	41.08 (10.11)	36.57(5.03)		
Min, Max	25.00, 93.00	23.00, 69.00		
Md (Q3-Q1)	41.00 (21.00)	33.00 (18.00)		

Note: N, number of PWS patients; SD, standard deviation; Md, median, Q1, first quartile; Q3, third quartile.

Table S3. Comparison of the average density of vessels (average vessels/skin area ratio) between PWS and healthy skin for 174 PWS patients by PAMB

Characteristics	Result
Average density of vessels for healthy skin (%)	
N (Missing)	174 (0)
Average (SD)	2.47 (1.05)
Min, Max	0.84, 4.76
Md (Q3-Q1)	2.14 (1.35)
Average density of vessels for PWS skin (%)	
N (Missing)	174 (0)
Average (SD)	14.50 (1.86)
Min, Max	4.28, 31.46
Md (Q3-Q1)	12.76 (6.75)
Difference between PWS and healthy skin (%)	
N (Missing)	174 (0)
Average (SD)	12.03 (1.27)
Min, Max	2.75, 16.58
Md (Q3-Q1)	10.15 (5.59)
Paired *t* value	13.17
P value	0.0000

Note: N, number of PWS patients; SD, standard deviation; Md, median, Q1, first quartile; Q3, third quartile.

Table S4. Comparison of the average diameter of vessels between PWS and healthy skin for 174 PWS patients by PAMB

Characteristics	Result
Average diameter of vessels for healthy skin (μm)	
N (Missing)	174 (0)
Average (SD)	22.47 (2.36)
Min, Max	12.52, 30.20
Md (Q3-Q1)	19.15 (6.10)
Average diameter of vessels for PWS skin (μm)	
N (Missing)	174 (0)
Average (SD)	109.14 (10.72)
Min, Max	45.30, 177.40
Md (Q3-Q1)	102.51 (46.42)
Difference between PWS and healthy skin (μm)	
N (Missing)	174 (0)
Average (SD)	86.67 (11.94)
Min, Max	10.15, 98.47
Md (Q3-Q1)	79.18 (49.71)
Paired *t* value	17.64
P value	0.0000

Note: N, number of PWS patients; SD, standard deviation; Md, median, Q1, first quartile; Q3, third quartile.

Table S5. Comparison of the maximum diameter of vessels between PWS and healthy skin for 174 PWS patients by PAMB

Characteristics	Result
Maximum diameter of vessels for healthy skin (μm)	
N (Missing)	174 (0)
Average (SD)	31.53 (5.36)
Min, Max	20.60, 56.85
Md (Q3-Q1)	27.76 (8.23)
Maximum diameter of vessels for PWS skin (μm)	
N (Missing)	174 (0)
Average (SD)	138.52 (14.51)
Min, Max	60.20, 196.70
Md (Q3-Q1)	121.95 (36.25)
Difference between PWS and healthy skin (μm)	
N (Missing)	174 (0)
Average (SD)	106.94 (15.16)
Min, Max	10.70, 128.95
Md (Q3-Q1)	96.54 (45.95)
Paired *t* value	21.51
P value	0.0000

Note: N, number of PWS patients; SD, standard deviation; Md, median, Q1, first quartile; Q3, third quartile.

Table S6. Comparison of the average depth of vessels between PWS and healthy skin for 174 PWS patients by PAMB

Characteristics	Result
Average depth of vessels for healthy skin (μm)	
N (Missing)	174 (0)
Average (SD)	430.00 (160.00)
Min, Max	336.00, 522.00
Md (Q3-Q1)	381.00 (85.00)
Average depth of vessels for PWS skin (μm)	
N (Missing)	174 (0)
Average (SD)	615.00 (195.00)
Min, Max	402.00, 893.00
Md (Q3-Q1)	578.00 (138.00)
Difference between PWS and healthy skin (μm)	
N (Missing)	174 (0)
Average (SD)	185.00 (102.00)
Min, Max	12.00, 331.00
Md (Q3-Q1)	203.00 (96.00)
Paired *t* value	19.00
P value	0.0000

Note: N, number of PWS patients; SD, standard deviation; Md, median, Q1, first quartile; Q3, third quartile.

Table S7. Comparison of the maximum depth of vessels between PWS and healthy skin for 174 PWS patients by PAMB

Characteristics	Result
Maximum depth of vessels for healthy skin (μm)	
N (Missing)	174 (0)
Average (SD)	510.00 (185.00)
Min, Max	371.00, 674.00
Md (Q3-Q1)	489.00 (286.00)
Maximum depth of vessels for PWS skin (μm)	
N (Missing)	174 (0)
Average (SD)	760.00 (235.00)
Min, Max	378.00, 1427.00
Md (Q3-Q1)	753.00 (441.00)
Difference between PWS and healthy skin (μm)	
N (Missing)	174 (0)
Average (SD)	250.00 (91.00)
Min, Max	59.00, 923.00
Md (Q3-Q1)	218.00 (75.00)
Paired *t* value	24.16
P value	0.0000

Note: N, number of PWS patients; SD, standard deviation; Md, median, Q1, first quartile; Q3, third quartile.

Table S8. Color types of clinical manifestations for 174 PWS patients

Color types		Number	Percentage	Effective percentage	cumulative percentage
Effectively	pink	63	36.21%	36.21%	36.21%
	purple	59	33.91%	33.91%	70.12%
	proliferative	52	29..88%	29..88%	100.00%
	Sum	174	100.00%	100.00%	

Table S9. Comparison of the average density of vessels (average vessels/skin area ratio) for 174 PWS patients with different color types by PAMB

Characteristics	Result
Number of vessels for pink lesion skin (%)	
N (Missing)	63 (0)
Average (SD)	6.71 (0.87)
Min, Max	4.28, 14.57
Md (Q3-Q1)	7.17 (3.58)
Number of vessels for purple lesion skin (%)	
N (Missing)	59 (0)
Average (SD)	14.69 (1.18)
Min, Max	6.58, 20.65
Md (Q3-Q1)	13.70 (5.49)
Number of vessels for proliferative lesion skin (%)	
N (Missing)	52 (0)
Average (SD)	23.73 (2.46)
Min, Max	10.25, 31.46
Md (Q3-Q1)	23.01 (8.61)

Note: N, number of PWS patients; SD, standard deviation; Md, median, Q1, first quartile; Q3, third

quartile.

Table S10. Comparison of the average diameter of vessels for 174 PWS patients with different color types by PAMB

Characteristics	Result
Average diameter of vessels for pink lesion skin (μm)	
N (Missing)	63 (0)
Average (SD)	68.39 (10.51)
Min, Max	45.30, 94.38
Md (Q3-Q1)	67.15 (16.56)
Average diameter of vessels for purple lesion skin (μm)	
N (Missing)	59 (0)
Average (SD)	113.35 (12.53)
Min, Max	55.54, 145.98
Md (Q3-Q1)	114.47 (20.55)
Average diameter of vessels for proliferative lesion skin (μm)	
N (Missing)	52 (0)
Average (SD)	153.72 (17.81)
Min, Max	62.32, 177.45
Md (Q3-Q1)	139.15 (34.73)

Note: N, number of PWS patients; SD, standard deviation; Md, median, Q1, first quartile; Q3, third quartile.

Table S11. Comparison of the maximum diameter of vessels for 174 PWS patients with different color types by PAMB

Characteristics	Result
Maximum diameter of vessels for pink lesion skin (μm)	
N (Missing)	63 (0)
Average (SD)	94.51 (12.16)
Min, Max	60.20, 120.65
Md (Q3-Q1)	90.57 (15.20)
Maximum diameter of vessels for purple lesion skin (μm)	
N (Missing)	59 (0)
Average (SD)	141.36 (15.08)
Min, Max	89.60, 161.74
Md (Q3-Q1)	133.58 (28.40)
Maximum diameter of vessels for proliferative lesion skin (μm)	
N (Missing)	52 (0)
Average (SD)	178.69 (19.75)
Min, Max	95.73, 196.70
Md (Q3-Q1)	174.51 (35.68)

Note: N, number of PWS patients; SD, standard deviation; Md, median, Q1, first quartile; Q3, third quartile.

Table S12. Comparison of the average depth of vessels for 174 PWS patients with different color types by PAMB

Characteristics	Result
Average depth of vessels for pink lesion skin (μm)	
N (Missing)	63 (0)
Average (SD)	455.00 (185.00)
Min, Max	402.00, 536.00
Md (Q3-Q1)	437.00 (46.00)
Average depth of vessels for purple lesion skin (μm)	
N (Missing)	59 (0)
Average (SD)	570.00 (190.00)
Min, Max	427.00, 697.00
Md (Q3-Q1)	558.00 (59.00)
Average depth of vessels for proliferative lesion skin (μm)	
N (Missing)	52 (0)
Average (SD)	865.00 (210.00)
Min, Max	485.00, 893.00
Md (Q3-Q1)	851.00 (78.00)

Note: N, number of PWS patients; SD, standard deviation; Md, median, Q1, first quartile; Q3, third quartile.

Table S13. Comparison of the maximum depth of vessels for174 PWS patients with different color types by PAMB

Characteristics	Result
Maximum depth of vessels for pink lesion skin (μm)	
N (Missing)	63 (0)
Average (SD)	580.00 (210.00)
Min, Max	378.00, 775.00
Md (Q3-Q1)	585.00 (128.00)
Maximum depth of vessels for purple lesion skin (μm)	
N (Missing)	59 (0)
Average (SD)	740.00 (220.00)
Min, Max	424.00, 940.00
Md (Q3-Q1)	725.00 (150.00)
Maximum depth of vessels for proliferative lesion skin (μm)	
N (Missing)	52 (0)
Average (SD)	1080.00 (240.00)
Min, Max	507.00, 1427.00
Md (Q3-Q1)	1045.00 (213.00)

Note: N, number of PWS patients; SD, standard deviation; Md, median, Q1, first quartile; Q3, third quartile.